

Control of Polarization Phase Offset in Low Threshold Polarization Switching VCSELs

Yan Zheng, Chin-Han Lin, *Student Member, IEEE*, and Larry A. Coldren, *Fellow, IEEE*

Abstract—Both polarization switching and control over the angle between polarization states is demonstrated. A novel dual intracavity contacted vertical-cavity surface-emitting laser utilizing asymmetric current injection is tested. Large extinction ratios >21 dB and a record-low threshold current of 0.19 mA is achieved for such devices. Control over the phase offset between two polarization states is accomplished by rotating current injection direction relative to the $\langle 110 \rangle$ axis. The phase offset between two polarization states is shown to follow a trigonometric function with maximum offsets along the $\langle 110 \rangle$ and $\langle \bar{1}\bar{1}0 \rangle$ directions and minimum offsets along the $\langle 100 \rangle$ and $\langle 010 \rangle$ directions.

Index Terms—Asymmetric current injection (ACI), molecular beam epitaxy, polarization, vertical-cavity surface-emitting lasers (VCSELs).

I. INTRODUCTION

VERTICAL-CAVITY surface-emitting lasers (VCSELs) have become key components in next-generation optical interconnects [1]. This is in part because VCSELs have shown many advantages such as higher reliability, yield, and their ability to be put into arrays. If the output polarization could be controlled, further opportunities in medical imaging [2], environmental monitoring [3], and military applications [4] could be explored. Although output polarization of VCSELs does not exhibit fundamental selection rules [5], several methods have been used to stabilize output polarization such as utilizing various mesa geometries [6], off-axis crystal surfaces [7], and surface gratings [8]. Several groups have also demonstrated asymmetric current injection (ACI) as a way to introduce gain anisotropies to control output polarization [9]–[11]. Although the carrier k -vectors are necessarily aligned with the substrate-normal (z -direction) at the absorption edge energy in quantum-wells, at lasing threshold and above, there is sufficient state filling to provide a significant lateral carrier momentum component which modifies the overall electron k -vector. Since there is a transition strength dependence between the electron k -vector and the incident electric field, a change in current direction can potentially control output polarization by influencing the transition strength (and thus gain) of specific polarizations.

Manuscript received October 07, 2010; revised November 11, 2010; accepted November 27, 2010. Date of publication December 10, 2010; date of current version February 24, 2011. This work was supported by the Defense Advanced Research Projects Agency (DARPA) through an STTR with ZIVA Corp.

The authors are with the University of California, Santa Barbara, Santa Barbara, CA 93106 USA (e-mail: yazheng@umail.ucsb.edu).

Color versions of one or more of the figures in this letter are available online at <http://ieeexplore.ieee.org>.

Digital Object Identifier 10.1109/LPT.2010.2098026

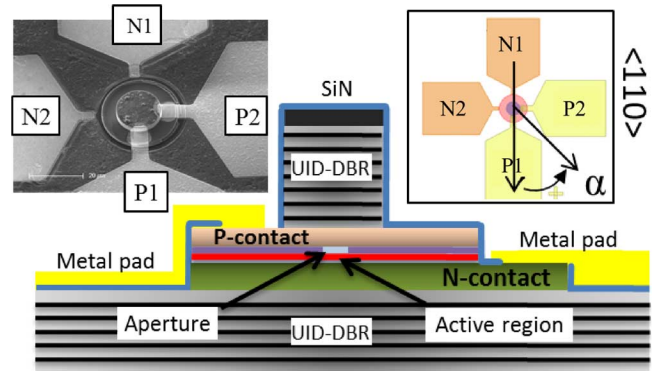


Fig. 1. Schematic of VCSEL epitaxial structure. Insets show top view of VCSEL contact-pads and its rotation angle α relative to the $\langle 110 \rangle$ axis and a corresponding SEM image.

In this letter we demonstrate switching between two orthogonal polarization states via asymmetric current injection utilizing a novel dual intracavity contacted circular mesa design. Control over polarization phase offset, or, the angle between polarization states, will also be shown by rotating current injection direction.

II. GROWTH AND FABRICATION

A dual intracavity design was used to avoid having to contact through a p-doped Distributed Bragg Reflector (p-DBR) top mirror which would have increased the current path length and decreased the carrier momentum lifetime through scattering events [12]. Moreover, traveling through the p-DBR unnecessarily adds more z -component to the carrier momentum vector that is isotropic with current direction. The p- and n-contact layers were thus grown close together to increase current directionality shown in Fig. 1. Molecular Beam Epitaxy (MBE) growth on (001)-cut undoped GaAs starts with 18 periods of unintentionally doped (UID) GaAs/AlAs to form the bottom DBR mirror followed by 420 nm of Si doped GaAs for the n-contact layer. The active region consists of three 8 nm thick $\text{In}_{0.2}\text{Ga}_{0.8}\text{As}$ quantum wells separated by 8 nm GaAs barriers. The active region was surrounded by a 30% AlGaAs separate confinement heterostructure (SCH). A linearly graded AlGaAs region then forms the oxide aperture. The free carrier absorption associated with the overlap between the optical field and the hole concentration is an important issue since the p-contact layer is placed so close to the active region. A modulation doping scheme was employed using multiple doping levels to minimize this overlap. In order to quickly and accurately supply all the doping levels, a custom Carbon Tetrabromide (CBr_4) carbon doping system was used [13]. The doping ranged from $1 \times 10^{18} \text{ cm}^{-3}$ to $4 \times 10^{18} \text{ cm}^{-3}$.

with the highly doped regions occurring at the optical nulls. The top mirror was composed of 32 periods of 85% AlGaAs/GaAs.

Circular mesas were created in a two-step dry-etching process that stops in the intracavity contact layers using a laser etch-monitor. The devices are then placed in a wet oxidation furnace to form the oxide aperture. A third etch removes the n-contact layer except from where the n-metal pads will be to help isolate orthogonal electron paths. A blanket SiN layer is then deposited and four equally spaced vias are opened around the mesa for metal contacts. Devices were rotated in various increments on the mask so that the output polarization can be studied as a function of current injection direction.

III. POLARIZATION SWITCHING

A linear polarizing lens is used to measure output polarization. The polarizer transmission axis is aligned to the 0° marker on the rotational lens mount. The $\langle 1\bar{1}0 \rangle$ axis of the wafer is then aligned to this marker. Output light intensity (LI) first passes through a microscope objective then the rotating polarizing lens and finally is measured by a Si photodetector.

Light-current-voltage (LIV) curves for a device with a mesa diameter of $13 \mu\text{m}$ and an aperture of $6 \mu\text{m}$ is shown in Fig. 2 for two polarization states. Asymmetric current injection was achieved by directing current between pads that face each other i.e. P1N1 or P2N2. The threshold current is 0.19 mA for both current configurations which is the lowest threshold reported for ACI polarization switching VCSEL. Output wavelength was 971 nm and the near field pattern uniformly filled the aperture with a diameter of roughly $13 \mu\text{m}$. When injecting current between the P1N1 pads, light output was found to be polarized close to 40° from the $\langle 110 \rangle$ axis. Probing the orthogonal P2N2 pads first showed lasing in the same polarization but quickly switches to the orthogonal polarization. This initial switching could be related to temperature effects [14]. At a polarizer angle of 120° shown in Fig. 2(b), the P2N2 direction initially lases aligned to 40° but switches to the orthogonal polarization after 0.37 mA. The preferred polarization angle is offset from the crystal axis due to misalignment of the polarizer to the current path. The ripples in the LI curves are a result of feedback from the substrate-air interface due to no anti-reflection (AR) coating. Small differences in wavelength between polarization states and thermal impedances of the two current paths slightly offset the oscillations in P1N1 to P2N2. The intensity and frequency of ripples in light output increases with decreasing device size and ultimately disappear under $1 \mu\text{s}$ pulsed conditions.

IV. POLARIZATION PHASE OFFSET

The phase offset between two polarization states was also investigated. Here we have defined the polarization state as the output polarization for a given current injection direction. The phase offset between two polarization states is the difference in polarizer angle between output power peaks.

LI curves were taken for every 20° rotation of the polarizer with either the P1N1 or P2N2 configuration probed. Light output of the device at a bias of 2 mA is plotted against the polarizer rotation angle to generate the polarization resolved output shown in Fig. 3. The measured data for the two orthogonal current injection configurations is fitted to a sine wave that has a R^2

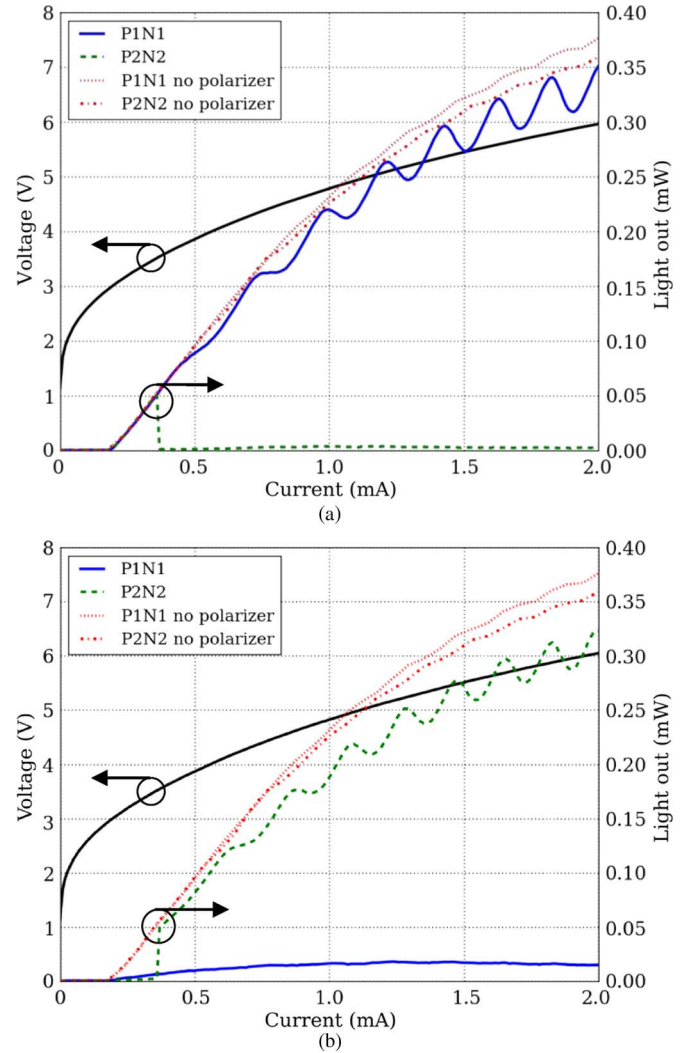


Fig. 2. L - I - V curve with polarizer transmission axis (a) 40° to the $\langle 1\bar{1}0 \rangle$ axis and (b) 120° to the $\langle 1\bar{1}0 \rangle$ axis.

value >0.999 . From the fit, the polarization rotational frequency was determined to be 2 rad^{-1} for both current directions. These two polarization states also showed a phase offset of approximately 90° .

From the good fit, extrapolated extinction ratios were obtained. The (P1N1)/(P2N2) state had an extinction ratio $>21 \text{ dB}$ at a polarizer angle of 38° and the (P2N2)/(P1N1) state had an extinction ratio $>25 \text{ dB}$ at a polarizer angle of 131° . These are one of the largest extinction ratios reported for a polarization switching VCSEL using ACI.

The circular structure of our VCSEL is a good platform to study the polarization dependence on current direction because its infinite rotational symmetry might allow one to see current injection effects independent of certain geometrical effects.

When injecting current along either the $\langle 110 \rangle$ or $\langle 1\bar{1}0 \rangle$ axis, past work with square VCSELs have reported phase offsets that vary randomly between 25° - 90° [9] or aligned to only the $\langle 110 \rangle$ or $\langle 1\bar{1}0 \rangle$ axes [15]. To test if our structure could better control the phase offset, VCSELs were rotated in the following angles (α), relative to the $\langle 110 \rangle$ direction: $[0^\circ, 22.5^\circ, 45^\circ, 90^\circ, 135^\circ,$

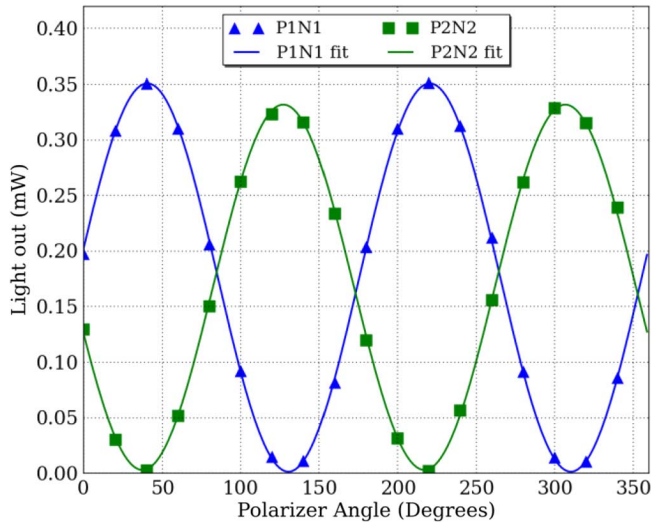


Fig. 3. Output power at 2.0 mA showing sinusoidal dependence to polarizer angle.

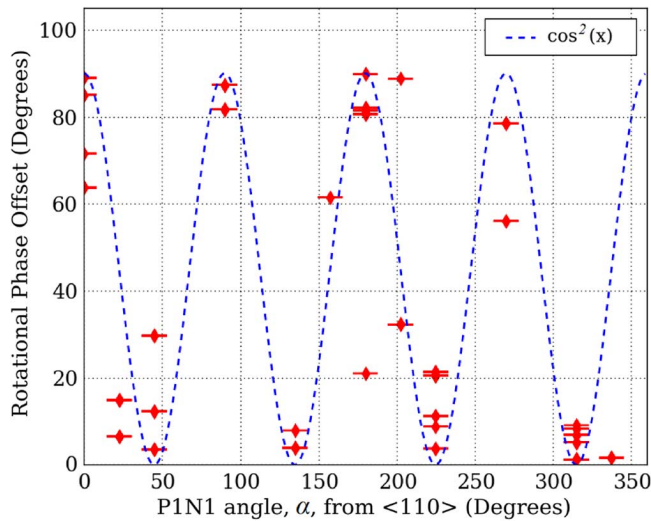


Fig. 4. Phase offsets between two polarization states measured as the current injection angle α is rotated.

157.5°, 180°, 202.5°, 225°, 270°, 315°, 337.5°] and phase offsets were calculated. These calculations were performed at biases that showed the best polarization switching performance.

We demonstrate in Fig. 4 control of polarization phase offset by rotating the current injection angle α . The measured data follows a $\cos^2(\alpha)$ dependence. The largest offsets between polarization states occurred every 90° with respect to the $\langle 110 \rangle$ axis. Minimal polarization phase offsets were found to occur when current was aligned to the $\langle 010 \rangle$ and $\langle 100 \rangle$ directions. This is related to the angle-dependent nature of the transition matrix element. Sopra *et al.* looked at birefringence in VCSELS [16] and showed that birefringence followed a similar trend. It is possible that other effects play complimentary roles in controlling polarization switching.

V. CONCLUSION

In this letter we have demonstrated a novel dual intracavity VCSEL capable of controlled switching between polarization

states by utilizing asymmetric current injection. Additional control over the offset between polarization states was also demonstrated. A reported threshold current of 0.19 mA is the lowest reported for a asymmetric current injection controlled polarization switching VCSEL. A high extinction ratio of >21 dB was also achieved between orthogonal polarization states. The output polarization was shown to fit a sinusoidal function with a polarization rotational frequency of 2 rad^{-1} .

ACKNOWLEDGMENT

The authors would like to thank Dr. M. Gross for his contributions.

REFERENCES

- [1] L. A. Coldren, Y. C. Chang, Y. Zheng, and C. H. Lin, "Efficient sources for chip-to-chip to box-to-box communication within data centers," in *Proc. IEEE Topical Meeting Series of the Photonics Society*, Playa del Carmen, Riviera Maya, Mexico, Jul. 2010, Paper TuD2.1.
- [2] S. L. Jacques, J. R. Roman, and K. Lee, "Imaging superficial tissues with polarized light," *Lasers Surgery Medicine*, vol. 26, no. 2, pp. 119–129, 2000.
- [3] M. Wang, "Aerosol polarization effects on atmospheric correction and aerosol retrievals in ocean color remote sensing," *Appl. Opt.*, vol. 45, no. 35, pp. 8951–8963, 2006.
- [4] C. S. L. Chun and F. A. Sadjadi, "Polarimetric laser radar target classification," *Opt. Lett.*, vol. 30, no. 14, pp. 1806–1808, Jul. 2005.
- [5] C. J. Chang-Hasnain, J. P. Harbison, G. Hasnain, A. C. v. Lehmen, L. T. Florez, and N. G. Stoffel, "Dynamic, polarization, and transverse mode characteristics of vertical cavity surface emitting lasers," *IEEE J. Quantum Electron.*, vol. 27, no. 6, pp. 1402–1409, Jun. 1991.
- [6] K. D. Choquette and R. E. Leibenguth, "Control of vertical cavity polarization with anisotropic transverse cavity geometries," *IEEE Photon. Technol. Lett.*, vol. 6, no. 1, pp. 40–42, Jan. 1994.
- [7] M. Takahashi, N. Egami, T. Mukaiyama, F. Koyama, and K. Iga, "Lasing characteristics of GaAs(311)A substrate based InGaAs–GaAs vertical-cavity surface-emitting lasers," *IEEE J. Sel. Topics Quantum Electron.*, vol. 3, no. 2, pp. 372–378, Apr. 1997.
- [8] J. M. Ostermann, P. Debernardi, and R. Michalzik, "Optimized integrated surface grating design for polarization-stable VCSELS," *IEEE J. Quantum Electron.*, vol. 42, no. 7, pp. 690–698, Jul. 2006.
- [9] L. M. Augustin, E. Smalbrugge, K. D. Choquette, F. Karouta, R. C. Strijbos, G. Verschaffelt, E.-J. Geluk, T. G. van de Roerand, and H. Thienpont, "Controlled polarization switching in VCSELS by means of asymmetric current injection," *IEEE Photon. Technol. Lett.*, vol. 16, no. 3, pp. 708–710, Mar. 2004.
- [10] Y. Sato, K. Furuta, and T. Katayama, "Polarization switching in vertical-cavity surface-emitting lasers by asymmetrical current injection," *IEEE Photon. Technol. Lett.*, vol. 20, no. 17, pp. 1446–1448, Sep. 1, 2008.
- [11] H. P. D. Yang, I. C. Hsu, F. I. Lai, G. Lin, H. C. Kuo, and J. Y. Chi, "Characteristics of cross-shaped polarization-switching vertical-cavity surface-emitting lasers for dual-channel communications," *Jpn. J. Appl. Phys.*, vol. 46, no. 14, pp. 326–329, 2007.
- [12] A. Haché, J. E. Sipe, and H. M. van Driel, "Quantum interference control of electrical currents in GaAs," *IEEE J. Quantum Electron.*, vol. 34, no. 7, pp. 1144–1154, Jul. 1998.
- [13] Y.-C. Chang, Y. Zhenga, J. H. English, A. W. Jackson, and L. A. Coldren, "Wide-dynamic-range, fast-response CBr4 doping system for molecular beam epitaxy," in *Proc. NAMBE*, Princeton, NJ, Aug. 9–12, 2009, Paper IX.5.
- [14] K. D. Choquette, D. A. Richie, and R. E. Leibenguth, "Temperature dependence of gain-guided VCSEL polarization," *Appl. Phys. Lett.*, vol. 64, p. 2062, 1994.
- [15] K. D. Choquette, R. P. Schneider, Jr., and K. L. Lear, "Gain-dependent polarization properties of vertical-cavity lasers," *IEEE J. Sel. Topics Quantum Electron.*, vol. 1, no. 6, pp. 661–666, Jun. 1995.
- [16] F. M. d. Sopra, M. Brunner, and R. Hovel, "Polarization control in strained T-bar VCSELS," *IEEE Photon. Technol. Lett.*, vol. 14, no. 8, pp. 1034–1036, Aug. 2002.